Available online at www.sciencedirect.com
SCIENCE DIRECT®
ELSEVIER
Nuclear Instruments and Methods in Physics Research A 547 (2005) 163–168
NUCLEAR INSTRUMENTS & METHODS IN PHYSICS RESEARCH Section A
www.elsevier.com/locate/nima

Hard-X-ray photoelectron spectroscopy of $Na_xCoO_2.yH_2O$

A. Chainani[a,*], T. Yokoya[b], Y. Takata[a], K. Tamasaku[c], M. Taguchi[a], T. Shimojima[b], N. Kamakura[a], K. Horiba[a], S. Tsuda[b], S. Shin[a,b], D. Miwa[c], Y. Nishino[c], T. Ishikawa[c], M. Yabashi[d], K. Kobayashi[d], H. Namatame[e], M. Taniguchi[e], K. Takada[f,g], T. Sasaki[f,g], H. Sakurai[f], E. Takayama-Muromachi[f]

[a]*Soft X-ray Spectroscopy Lab, RIKEN/SPring-8, 1-1-1 Kouto, Mikazuki-cho, Sayo-gun, Hyogo 679-5148, Japan*
[b]*Institute for Solid State Physics, University of Tokyo, Kashiwa,Chiba 277-8581, Japan*
[c]*Coherent X-ray Optics Lab, RIKEN/SPring-8, 1-1-1 Kouto, Mikazuki-cho, Sayo-gun, Hyogo 679-5148, Japan*
[d]*JASRI/SPring-8, 1-1-1 Kouto, Mikazuki-cho, Sayo-gun, Hyogo 679-5198, Japan*
[e]*HiSOR, Hiroshima University, Higashi-Hiroshima 739-8526, Japan*
[f]*National Institute for MaterialsScience, Tsukuba, Ibaraki, 305-0044, Japan*
[g]*CREST, Japan Science and Technology Corporation, Japan*

Available online 13 June 2005

Abstract

We study the bulk electronic structure of $Na_xCoO_2.yH_2O$ using Hard X-ray (HX, $h\nu = 5.95$ KeV) synchrotron photoelectron spectroscopy (PES). The Co 2*p* core level spectra show well-separated Co^{3+} and Co^{4+} ions. Cluster calculations suggest low spin Co^{3+} and Co^{4+} character, and a moderate on-site Coulomb correlation energy U_{dd}~3–5.5 eV. Photon-dependent valence band PES identifies Co 3*d* and O 2*p* derived states, in near agreement with band structure calculations. We discuss the importance of HX-PES for studying correlated transition metal oxides.

PACS: 74.25.jb; 74.25.kc; 79.60.−i

Keywords: Hard X-ray photoelectron spectroscopy; Cobaltates; Superconductivity; Correlated electrons

Superconductivity in the hydrated Co-oxide system $Na_xCoO_2.yH_2O$ seems to resemble doping-induced superconductivity as in high-T_c cuprates [1]. The cobaltates are also layered materials, possessing CoO_2 layers consisting of (CoO_6) octahedra. The Na^{1+} content x corresponds to Co^{3+} valency in a matrix of Co^{4+} ions. Further, in spite of extensive investigations [2], it has not been possible to achieve superconductivity in a 3-dimensional Co-oxide system. Electron–electron correlations between Co 3*d* electrons is believed to

*Corresponding author.
E-mail address: chainani@spring8.or.jp (A. Chainani).

0168-9002/$ - see front matter © 2005 Elsevier B.V. All rights reserved.
doi:10.1016/j.nima.2005.05.021

be substantial (on-site Coulomb energy, U_{dd} = 3–5.5 eV) from electron spectroscopic studies [3–7], albeit less than copper oxides (U_{dd} = 5–8 eV, Ref. [8]). Theoretical studies [9–12] including resonating-valence-bond models, predict fascinating properties for this system. Recent experiments on such cobaltates show dimensional crossover [13] and the relation of spin entropy with the large thermopower [14] in the non-superconducting compositions.

Since the doping-dependent T_c's are rather low [15], with a maximum T_c of ~5 K, conventional phonon-mediated superconductivity also needs to be carefully investigated for the Co-oxide superconductors. The layered Co oxides thus provide a new opportunity to study charge and spin dynamics in superconducting oxides. Recent studies indicate that Na_xCoO_2 is close to charge and spin ordering tendencies [16,17]. NMR studies [18] on non-superconducting Na_xCoO_2 have concluded integral valent Co^{3+} and Co^{4+} ions reflecting charge order. Also, while intercalated water is necessary for superconductivity, its role in modifying the electronic structure is not yet clear. It is thus important to study the electronic structure of $Na_xCoO_2.yH_2O$ as a function of Na content, x and water content, y.

Photoelectron spectroscopy (PES) provides a reliable description of the electronic structure of transition metal compounds [3–8] based on the Zaanen–Sawatzky-Allen (ZSA) phase diagram [19]. Core-level PES provides valence states and an estimate of electronic structure parameters: on-site Coulomb energy (U_{dd}), charge-transfer (CT) energy (Δ) and hybridization strength (V). Further, while angle-resolved (AR) valence band (VB) PES is necessary to study experimental band structure, angle integrated VB-PES provides the transition probability modulated density of states (DOS). The surface sensitivity of PES has often led to controversies regarding surface versus bulk electronic structure, and hence, hard X-ray(HX)-PES, resonant Auger spectroscopy and site-selective PES are very important and promising [20–26]. The development of HX-PES with a resolution of 240 meV, which has been recently improved to a resolution of 75 meV, at a kinetic energy of 5.95 KeV, is a valuable advance for investigating bulk electronic structure of materials [27]. Its usefulness in the study of semiconductors has also been demonstrated [27]. The principal advantage of HX-PES is the high escape depth of emitted photoelectrons [28], enabling a truly bulk measurement. At $h\nu = 5.95$ KeV, the escape depth for Co 2p and O 1s electrons is estimated to be ~50 Å, significantly larger than that with soft X-ray photons from a Mg- or Al–Kα source(~10 Å) [28]. Since photo-ionization cross-sections (PICS) become very low at high photon energies [29], VB studies at $h\nu \geqslant 5$ keV were very difficult earlier, although the first core level study using 8 keV photons was done nearly 30 years ago [30].

We study VB and core-level HX-PES ($h\nu = 5.95$ KeV) of the Co oxide superconductor, $Na_{0.35}CoO_2.1.3H_2O$, as well as non-superconducting $Na_{0.7}CoO_2$ and CoO. Co 2p core level spectra show well defined Co^{3+} and Co^{4+} features in the normal phase of $Na_{0.35}CoO_2.1.3H_2O$. Cluster calculations indicate a moderate U_{dd}~3–5.5 eV. The VB spectra consisting of Co 3d and O 2p derived states are compared with soft X-ray ($h\nu$ = 700 eV) PES and reported band structure calculations (BSCs). The VB is similar for both compositions on the energy scale of the resolution used, suggesting important modifications only at a lower energy scale near the Fermi level(E_F) [13], probably related to confined carriers in CoO_2 layers and/or a modified electron–phonon coupling.

Polycrystalline samples of $Na_{0.35}CoO_2.1.3H_2O$ and $Na_{0.7}CoO_2$ were made and characterized as described in Ref. [1]. Magnetization measurements confirmed the bulk T_c of 4.5 K for $Na_{0.35}CoO_2.1.3H_2O$. The retention of water under vacuum conditions was ensured by using freshly prepared samples mounted on substrates with silver paste and also covered with it. After transferring samples to the measurement chamber and cooling to 100 K, they were scraped in situ with a diamond file to obtain clean surfaces. The samples were then cooled to 15 K for HX-PES measurements, at a vacuum of 1×10^{-10} Torr. HX-PES was performed at undulator beam line BL29XU, Spring-8 (Ref. [31]) using 5.95 KeV photons and a modified SES2002 electron analyzer. For the present measurements, the energy

width of incident X-rays was 70 meV, and the total energy resolution, ΔE was set to ~ 0.5 eV. Soft X-ray PES ($h\nu = 700$ eV) was performed at BL19B, KEK, PF, using a CLAM4 electron analyzer with $\Delta E \sim 0.3$ eV. Samples were cooled to 30 K and the vacuum was 8×10^{-10} Torr during measurements. Single crystal CoO was scraped insitu and measured at 300 K. E_F of gold was also measured to calibrate the energy scale.

The Co $2p$ core level PES spectra of $Na_{0.35}CoO_2.1.3H_2O$, $Na_{0.7}CoO_2$ and CoO obtained using $h\nu = 5.95$ KeV photons are shown in Fig. 1. The Co 2p spectrum of $Na_{0.35}CoO_2.1.3H_2O$ exhibits main peaks derived from Co $2p_{3/2}$ and $2p_{1/2}$ due to spin-orbit splitting, and two satellites at $\sim$10 eV higher binding energy (BE) from the main peaks. The $2p_{3/2}$ peak itself consists of two peaks. This is also seen in the $2p_{1/2}$ region with well-separated peaks in raw spectra. A simple interpretation is that the low BE peak is due to Co^{3+} and the high BE peak is due to Co^{4+} states. In Fig. 2 we overlay a least-squares curve fit on the data of $Na_{0.35}CoO_2.1.3H_2O$ and $Na_{0.7}CoO_2$, obtained using asymmetric Voigt functions and a Shirley background. The fits resolve contributions of Co^{3+} and Co^{4+} features in the main peaks, as seen in the decomposition. We used a single feature for the satellites for simplicity. The peak widths for Co^{4+} feature and satellite in $Na_{0.7}CoO_2$ are broader than in $Na_{0.35}CoO_2.1.3H_2O$, suggesting larger inhomogeneity in valency due to

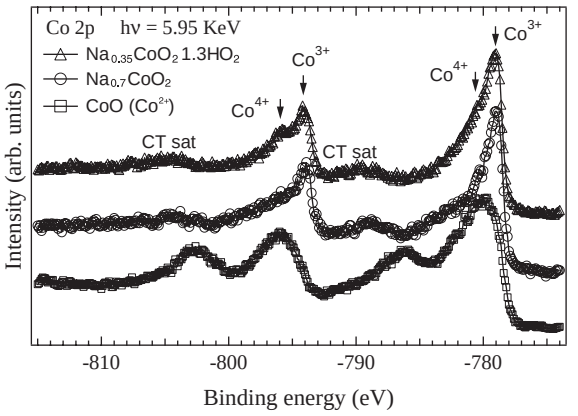

Fig. 1. Co 2p core level PES spectra of $Na_{0.35}CoO_2.1.3H_2O$, $Na_{0.7}CoO_2$ and CoO obtained using $h\nu = 5.95$ KeV photons.

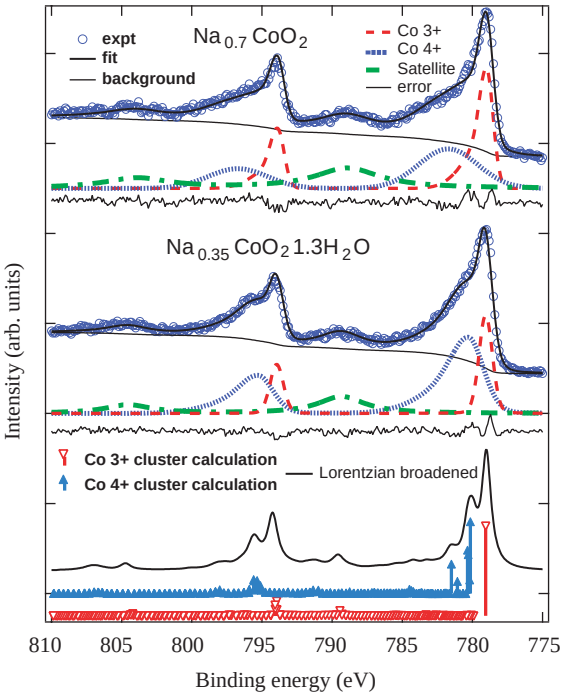

Fig. 2. A least-squares curve fit to the Co 2p spectrum of $Na_{0.35}CoO_2.1.3H_2O$ and $Na_{0.7}CoO_2$, shows contributions of Co^{3+} and Co^{4+} states in the $2p_{3/2}$ and $2p_{1/2}$ main peaks, with a single peak assumed for satellites. Line diagrams show calculated low-spin Co^{3+} and Co^{4+} states. For $Na_{0.35}CoO_2.1.3H_2O$, the calculated spectra obtained by broadening the discrete states are also shown, in fair agreement with the data

increased Na doping. We have also confirmed that the crystal structure analysis of both samples indicated absence of impurity phases within experimental accuracy. Further, we have carefully checked that BE's for Co^{3+} main peaks are actually lower than the corresponding peaks of Co^{2+} in CoO, e.g. $2p_{3/2}$ peak is at 779.0 and 780.0 eV, respectively (1). The CoO spectra match those obtained with a MgKα source extremely well in BE and spectral shapes [3,7].

Well-separated core-level features are observed in charge-density wave (CDW) systems[32] as well as intermediate valence materials without static charge order [33], because PES is a fast probe. Earlier work on 3-dimensional perovskite oxides $La_{1-x}Sr_xCoO_3$ ($x = 0.0$–0.4) showed essentially a single peak at the same BE, and no clear

separation into Co^{3+} and Co^{4+}states [4,5]. The peak width broadened initially with doping for $x = 0.1$, but across the semiconductor–metal transition at $x = 0.2$ in $La_{1-x}Sr_xCoO_3$, the peaks became narrower for increasing x due to uniform non-integral valency at Co-sites [4]. Surprisingly, for oxide systems which show charge-ordering or disproportionation, such as $Pr_{0.5}Sr_{0.5}MnO_3$, perovskite ferrites, etc. well-separated integral valence features are not observed [34,35]. It is due to the ground state being dominated by a CT $d^{n+1}L^1$ (L is a ligand hole) rather than a d^n configuration, based on model Hamiltonian cluster calculations [35]. From similar cluster calculations (details are described in Ref. [36] and results of one such calculation for low spin Co^{3+} and Co^{4+} are shown as line diagrams in Fig. 2), we obtain the electronic structure parameters of $U_{dd} = 5.5\,eV$, $\Delta = 4.0\,eV$ and $V = 3.1 \pm 0.2\,eV$ which describe the Co $2p$ spectral features fairly well. For simplicity, we use the same parameter values for Co^{3+} and Co^{4+} except for crystal field splitting, 10Dq. The 10Dq values for Co^{3+} and Co^{4+} are 2.5 and 4.0 eV, respectively. The uncertainty in Δ is $\pm$ 0.5 eV while the calculated spectra were very similar for $U_{dd} = 3.0$–$5.5\,eV$, consistent with earlier work [3–7]. The ground state character for Co^{3+} is $3d^6 = 57.0\%$, $3d^7L^1 = 38.1$ % and $3d^8L^2 = 4.9$ %, while that for Co^{4+} is $3d^5 = 57.4$ %, $3d^6L^1 = 37.6$ % and $3d^7L^2 = 5.0$ %. We have also checked for high-spin Co^{3+} and Co^{4+} configurations but the results are not compatible with the data. The analysis suggests that $Na_{0.35}CoO_2.1.3H_2O$ and $Na_{0.7}CoO_2$ contain low spin Co^{3+} and Co^{4+} configurations, consistent with magnetic measurements [17]. The calculations also show CT character of the satellites. The results indicate an electronic structure of mixed character, but more Mott–Hubbard-like rather than CT-like in terms of the ZSA phase diagram.

While the main peaks of Co^{3+} and Co^{4+} features are well separated, it is clear from the cluster calculations that Co $2p$ spectra consist of degenerate multiple features at higher BEs. The satellite intensity as estimated from the curve fits is also large, it being ~70% of the Co^{3+} main peak. This is in fair agreement with the calculated spectra as is shown for $Na_{0.35}CoO_2.1.3H_2O$ in Fig. 2, obtained by a Lorentzian broadening of the discrete states. However, it is difficult to estimate the actual Co^{3+} : Co^{4+} relative concentrations although the main peak intensities are roughly consistent (within 10%) compared to the nominal concentrations. The present studies are consistent with integral valent charge order measured by NMR studies [18]. Although LDA + U calculations [16] for $Na_{0.33}CoO_2$ indicate a correlation driven charge order with a ferromagnetic ground state, the absence of ferromagnetic order and suppression of Co moments on introducing water in $Na_{0.35}CoO_2.1.3H_2O$ (Ref. [37]) suggests an additional input to the electronic structure, most likely strong electron–phonon coupling as in regular CDW transitions.

The HX-PES VB spectra of $Na_{0.35}CoO_2.1.3H_2O$, $Na_{0.7}CoO_2$ and CoO are shown in Fig. 3, along with the soft X-ray ($h\nu = 700\,eV$) spectrum of $Na_{0.35}CoO_2.1.3H_2O$. For $Na_{0.35}CoO_2.1.3H_2O$, the HX-PES spectrum shows a low intensity peak at 0.9 eV and a broad structure centered around 6 eV. In comparison, the $h\nu = 700\,eV$ spectrum shows a higher intensity 0.9 eV peak with the leading edge crossing E_F and a broad peak centered at 5 eV(data normalized at 5 eV BE). The spectral changes for the two photon energies arise from changes in PICS. This is

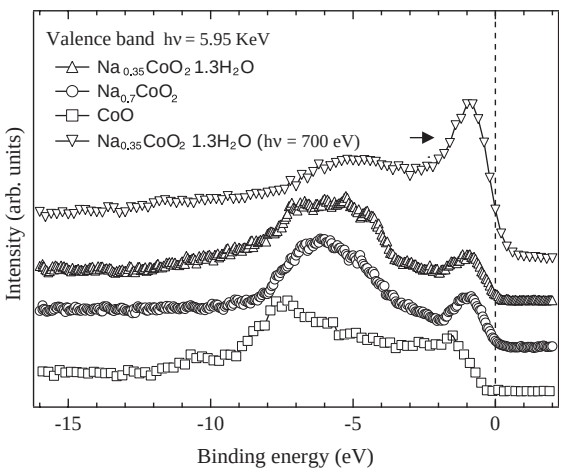

Fig. 3. Valence band HX-PES ($h\nu = 5.95\,KeV$) spectra of $Na_{0.35}CoO_2.1.3H_2O$, $Na_{0.7}CoO_2$ and CoO, and of $Na_{0.35}CoO_2.1.3H_2O$ obtained using $h\nu = 700\,eV$ photons. The Co 3d states are enhanced in the $h\nu = 700\,eV$ spectrum.

confirmed by comparing the present HX-PES CoO data with that reported in Ref. [38] for $h\nu = 600$ eV. The spectral intensity changes and comparison with BSCs (Ref. [39]) indicate that the feature at 0.9 eV is due to Co 3*d* states and the broad peak centered at 5–6 eV is dominated by O 2*p* states. The observed relative intensity changes indicate deviations from available calculated atomic PICS at $h\nu = 8.0$ KeV [29] which suggest the higher relative intensity of the Co 3*d* states compared to O 2*p* states. BSCs for $Na_{0.5}CoO_2$ indicate a peak closer to E_F, with high DOS at E_F derived from Co 3*d* t_{2g} states, which is separated from the Co 3*d* e_g states located in the unoccupied states [39]. While oxides can show a contamination peak around 10 eV, the feature at 10.5 eV in CoO is intrinsic as it is observed for cleaved single crystals [7,38] and in the present case. It is clearly absent in $Na_{0.7}CoO_2$. A weak tailing feature between 9 and 12 eV is observed in $Na_{0.35}CoO_2.1.3H_2O$. Comparing with studies on interaction of water with a high-T_c cuprate [40] and its absence in $Na_{0.7}CoO_2$, we attribute it to the water present in $Na_{0.35}CoO_2.1.3H_2O$. The O 1s spectra also indicate the presence of a water-derived signal only in the superconducting composition [41]. It is also noted that the Co 3*d* and O 2*p* derived states are similar in $Na_{0.35}CoO_2.1.3H_2O$ and $Na_{0.7}CoO_2$. The VB of CoO shows a feature at nearly 1.6 eV consisting of Co 3*d* states and a higher BE broad feature due to O 2*p* states at about 7 eV. A comparison indicates that in $Na_{0.35}CoO_2.1.3H_2O$ and $Na_{0.7}CoO_2$, the Co 3*d* feature is shifted to lower BE compared to CoO, as in Co 2*p* core levels (Fig. 1).

Recent high-resolution ARPES studies on non-superconducting $Na_xCoO_2 (x = 0.5–0.7)$ also suggest consistency with BSCs, but with a renormalization of electronic states on a low energy scale of 100 meV [13,42]. This energy scale is beyond present HX-PES measurements. A more accurate analysis at and very near E_F in superconducting $Na_{0.35}CoO_2.1.3H_2O$ requires higher resolution measurements, preferably with ARPES, to obtain the energy and momentum resolved electronic structure. The interplay of electron–electron correlations and strong electron–phonon coupling [43] of renormalized carriers in $Na_{0.35}CoO_2.1.3H_2O$ could stabilize a 'composite glue' for pairing, driven by a change in hybridization or intersite Coulomb interactions.

The present study shows that the bulk electronic structure of correlated oxides can be reliably obtained using HX-PES. We have recently applied HX-PES to also investigate: (i) the Mott–Hubbard transition in V_2O_3 as a function of temperature [44], (ii) the composition controlled semiconductor–metal transition in colossal magneto-resistance manganites [45], and (iii) the chemical potential shift in the high-T_c cuprates [46]. These studies show the enormous potential of HX-PES in studying correlated electron systems.

In conclusion, HX-PES provides the bulk electronic structure of $Na_xCoO_2.yH_2O$. In contrast to 3-dimensional-doped Co oxides, the Co 2*p* core level spectra show well-separated Co^{3+} and Co^{4+} ions. Cluster calculations suggest low spin Co^{3+} and Co^{4+} states, and a moderate on-site U_{dd} ~3–5.5 eV. Valence band PES identifies Co 3*d* and O 2*p* derived states, nearly in agreement with BSCs.

AC thanks Professor O. Gunnarsson for very valuable discussions. We thank Drs. M. Arita, T. Tokushima and K. Shimada for valuable experimental support.

References

[1] K. Takada, H. Sakurai, E. Takayama-Muromachi, F. Izumi, R. Dilanian, T. Sasaki, Nature 422 (2003) 53.
[2] J.B. Goodenough, in Progress in: H. Reiss(Ed.) Solid State Chemistry, Vol.5 Pergamon, London, 1971, p. 145;
M. Imada, A. Fujimori, Y. Tokura, Rev. Mod. Phys. 70 (1998) 1039.
[3] J. van Elp, J.L. Wieland, H. Eskes, P. Kuiper, G.A. Sawatzky, F.M.F. de Groot, T.S. Turner, Phys. Rev. B 44 (1991) 6090.
[4] A. Chainani, M. Mathew, D.D. Sarma, Phys. Rev. B 46 (1992) 9976.
[5] T. Saitoh, A.E. Bocquet, T. Mizokawa, A. Fujimori, Phys. Rev. B 52 (1995) 7934;
T. Saitoh, T. Mizokawa, A. Fujimori, M. Abbate, Y. Takeda, M. Takano, Phys. Rev. B 56 (1997) 1290.
[6] T. Mizokawa, L.H. Tjeng, P.G. Steeneken, N.B. Brookes, I. Tsukada, T. Yamamoto, K. Uchinokura, Phys. Rev. B 64 (2001) 115104.

[7] F. Parmigiani, L. Sangaletti, J. Electron Spectrosc. Relat. Phenom. 98–99 (1999) 287.
[8] A. Fujimori, E. Takayama-Muromachi, Y. Uchida, B. Okai, et al., Phys. Rev. B 35 (1987) 8814;
Z.-X. Shen, J.W. Allen, J.J. Yeh, J.-S. Kang, W. Ellis, W. Spicer, I. Lindau, M.B. Maple, Y.D. Dalichaouch, M.S. Torikachvili, J.Z. Sun, T.H. Geballe, Phys. Rev. B 36 (1987) 8414;
H. Eskes, L.H. Tjeng, andG.A. Sawatzky, Phys. Rev. B 41 (1990) 288.
[9] G. Baskaran, Phys. Rev. Lett. 91 (2003) 097003.
[10] B. Kumar, B.S. Shastry, Phys. Rev. B 68 (2003) 104508.
[11] Q.-H. Wang, D.-H. Lee, P.A. Lee, Phys. Rev. B 69 (2004) 092504.
[12] W. Koshibae, S. Maekawa, Phys. Rev. Lett. 91 (2003) 257003.
[13] T. Valla, et al. Nature 417 (2002) 627.
[14] Y. Wang, N.S. Rogado, R.J. Cava, N.P. Ong, Nature 423 (2003) 425.
[15] R.E. Schaak, T. Klimczuk, M.L. Foo, R.J. Cava, Nature 424 (2003) 527.
[16] J. Kunes, K.-W. Lee, W. Pickett, Phys. Rev B 70 (2004) 045104.
[17] I. Terasaki, Physica B 328 (2003) 63.
[18] R. Ray, A Ghoshray, K. Ghoshray, S. Nakamura, Phys. Rev. B 59 (1999) 9454;
J.L. Gavilano, D. Rau, B. Pedrini, J. Hinderer, H.R. Ott, S. Kazakov, J. Karpinski, Phys. Rev B 69 (2004) 100404.
[19] J. Zaanen, G.A. Sawatzky, J.W. Allen, Phys. Rev. Lett. 55 (1985) 418.
[20] L. Braicovich, N.B. Brookes, C. Dallera, M. Salvietti, G.L. Olcese, Phys. Rev. B 56 (1997) 15047.
[21] J. Woicik, E.J. Nelson, L. Kronik, M. Jain, J.R. Chelikowsky, D. Heskett, L.E. Berman, G.S. Herman, Phys. Rev. Lett 89 (2002) 077401.
[22] J. Danger, et al. Phys.Rev. Lett 88 (2002) 243001.
[23] S. Thiess, C. Kunz, B.C.C. Cowie, T.L. Lee, M. Renier, J. Zegenhagen, Solid State Communications 132 (2004) 589.
[24] W. Drube, T. Eickhoff, H. Schulte-Schrepping, J. Heuer, AIP Conf.Proc. 705 (2004) 1130.
[25] C. Dallera, L. Duo, L. Braicovich, G. Pannaccione, G. Paolicelli, B. Cowie, J. Zegenhagen, Appl. Phys. Lett. 85 (2004) 4532.
[26] P. Torelli, et al. Rev. Sci. Instrum. 76 (2005) 023909.
[27] K. Kobayashi, et al., Appl. Phys. Lett. 83 (2003) 1005;
Y. Takata, et al., Appl. Phys. Lett. 84 (2004) 4310
Y.Takata, et al., Nucl. Instr. Meth. A, in this issue.
[28] NIST Electron Inelastic Mean Free Path Database: Ver 1.1.(2000).
[29] J.J. Yeh, I. Lindau, At. Data Nucl. Data Tables 32 (1985).
[30] I. Lindau, P. Pianetta, S. Doniach, W.E. Spicer, Nature 250 (1974) 214.
[31] K. Tamasaku, Y. Tanaka, M. Yabashi, H. Yamazaki, N. Kawamura, M. Suzuki, T. Ishikawa, Nucl. Instr. Meth. A 467/468 (2001) 686.
[32] T.E. Kidd, T. Miller, T.-C. Chiang, Phys. Rev. Lett. 83 (1999) 2789.
[33] P.G. Steeneken, et al. Phys. Rev. Lett. 90 (2003) 247005.
[34] E.Z. Kurmaev, et al. Phys. Rev. B 59 (1999) 12799.
[35] A.E. Bocquet, et al. Phys. Rev. B 45 (1992) 1561.
[36] M. Taguchi, T. Uozumi, A. Kotani, J. Phys. Soc. Jpn. 66 (1997) 247.
[37] R. Jin, B.C. Sales, P. Khalifah, D. Mandrus Phys. Rev. Lett. 91 (2003) 217001.
[38] G. Ghiringhelli, et al., Phys. Rev. B 66 (2002) 075101.
[39] D.J. Singh, Phys. Rev. B 61 (2000) 13397;
D.J. Singh, Phys. Rev. B 68 (2003) 020503 (R).
[40] S.L. Qiu, et al., Phys. Rev. B 37 (1988) 3747.
[41] A. Chainani, et al. Phys. Rev. B 69 (2004) R180508.
[42] M.Z. Hasan, et al. Phys. Rev. Lett. 92 (2004) 246402;
H.-B. Yang, et al. Phys. Rev. Lett. 92 (2004) 246403.
[43] O. Rosch, O. Gunnarsson, Phys. Rev. Lett. 92 (2004) 146403.
[44] N. Kamakura, et al., Europhys. Lett. 68 (2004) 557.
[45] K. Horiba, et al, Phys. Rev. Lett. 93 (2004) 236401.
[46] M. Taguchi, et al. cond-mat/0501621